Computer Integrated Surgery II: Literature Evaluation
Group 1: Motorized Fixation to Tubular Retractor
Caroline Hoerrner
choerrn1@jhu.edu

Project Overview

_____Our project aims to improve the usage of tubular retractors in deep lesion brain surgery. Tubular retractors are quickly becoming the gold standard in brain lesion resection. However, they offer a smaller operating field than their classical counterparts, and frequently require repositioning during procedures. Specifically in deeper lesions, the long, rigid tube design can be difficult to maneuver and reposition within the brain, motivating invention of a motorized fixation that increases the precision and accuracy of the retractor repositioning process. We aim to motorize the angulation of the retractor using an orientation tracking wand (eventually retrofitted onto a microsurgical forcep) to allow the surgeon intuitive control of the retractor angle.

Papers Selected

For this evaluation, I have chosen three different papers addressing different elements of our design process. I first chose “Frameless Stereotactic Insertion of Viewsite Brain Access System with Microscope-Mounted Tracking Device for Resection of Deep Brain Lesions: Technical Report,” as this paper outlines a clear use case for our design. It highlights prominent features of the deep target resection procedure, and notes limitations of tubular retractors. Next, I selected “Forces exerted during microneurosurgery: a cadaver study.” This paper provides quantifiable data to characterize the forces experienced by various brain tissue during routine microneurosurgical procedures. Finally, the paper “Improving the Precision and Speed of Euler Angles Computation from Low-Cost Rotational Sensor Data” provides an analysis of rotation representation methods as they optimize precision and speed in gyroscope readings. This will be crucial in maximizing the accuracy of our IMU data.

Insertion of Viewsite Brain Access System with Microscope-Mounted Tracking Device

This paper details an improved technical approach to minimally invasive deep target lesion resection. The surgeons make use of many different advancements in minimally invasive brain surgery including the tubular retractor, offering our project valuable insight into the current limitations of these procedures.

In the three cases outlined, the surgeons combine use of the VBAS tubular retractor system with neuronavigation and surgical microscopes to create a seamless workflow that minimizes parenchymal damage. While neuronavigation is common in deep lesion resection to guide surgical approach, and surgical microscopes are also common in these procedures, they are not often used together. This is because these technologies do not interface well, resulting in a lot of back and forth for the surgeon. In

the approach used by White et al., the surgeon makes use of the focus locking capability of the Leica microscope to utilize neuronavigation while minimizing time away from the surgical microscope. The operative set up is outlined below.

Image sourced from White, et al.

The minimal parenchymal damage and lack of postoperative neurological complications in all three cases show the success of the combined surgical technique in achieving minimally invasive tumor evacuation. This provides greater support for the use of neuronavigation in all similar procedures, suggesting the potential for innovation in robotic auto positioning in the near future.

This sets clear standards for the best use cases of tubular retractors in similar procedures, and highlights major limitations on their usefulness. The authors note that mobility of the tubular retractor can be useful in resection of larger masses, and stiff anchoring of the tubular retractor can sometimes limit the surgical field of view. They also note that longer retractors used in deeper lesions can be difficult to manver and achieve optimal use angle.

This provides motivation to create a new system that allows for precise angulation of the tubular retractor to provide the surgeon with greater control.To achieve optimal results, retractor positioning must interface seamlessly without the need of the surgeon to look up from the microscope. Successful precision motorization of the tubular retractor has far greater implications on the use of auto-focusing in neuronavigation.

While this paper provides a strong motivational foundation for the core concept of our design, it lacks key numerical data to assert the improved outcome of patients. The authors also fail to identify potential sources of trauma introduced during the procedure (or, rather, sources specifically not introduced that would have been given other

methodology). They also fail to elaborate on the need for repositioning retraction during the course of the procedure, and the act of repositioning is often merely implied.

Overall, the paper offers key insight into the future gold standard of deep target lesion resection. However, the authors could have improved the validity of their methodology by introducing more cases and offering some numerical value (e.g. operating time, recovery time) to assert why their approach is an improvement on previous procedures.

Forces Exerted During Microneurosurgery

In this study, the authors explore the forces exerted on brain tissue during robot assisted neurosurgical procedures. This gives a clear sense of the baseline trauma endured during resection procedures, offering us goalposts to meet in terms of the forces created during retractor readjustment.

Our initial goal to motorize the movement of the tubular retractor to increase accuracy and maneuverability operates under the assumption that any motorized movement will offer a decreased resistance force to the repositioning that would have otherwise occurred by hand. However, in order to clear our prototype for clinical use (if that were to happen in the future), more comprehensive force analysis would need to be performed. This force testing is included in the established maximum goal to implement safety features to limit velocity and maximum angle of motion (see project proposal).

The paper found differences between the average force generated from several different standard procedures in robotic neurosurgery, and attempts to ascertain average force values that differentiate injury and non-injury causing maneuvers. This fills a critical gap in literature on quantitative evaluations of forces in these procedures.

To perform this task, the experimenters fitted a force/torque sensor between the end effector of a 6 DOF robot arm and surgical tool holder. They then completed several iterations of incision, retractions, and dissections in various parts of the brain and analyzed the accompanying force readings. The average force data can be seen below.

The major takeaways were that the average force to retract brain tissue 5mm was greater than the force of either incision type (0.08 N compared to 0.01N and 0.05N). It was also noted that the forces needed to manipulate the brainstem were generally greater in the forces needed to manipulate the cerebellum or cerebrum (0.05N compared to 0.2N or 0.013N).

Table 1. The median (interquartile range) of forces exerted (Newton) when performing simple procedures in different brain regions

		Median (interquartile range)		
		Stab Incision	Carrying Incision	Retraction
Cerebrum (n = 24)	Gyrus rectus (n = 8)	<0.01 (0.00 – 0.03)	0.02 (0.01 – 0.03)	0.03 (0.03 – 0.05)
	Inferior temporal gyrus (n = 8)	<0.01 (0.00 – 0.01)	0.02 (0.00 – 0.03)	0.07 (0.06 – 0.09)
	Middle frontal gyrus (n = 8)	<0.01 (0.00 – 0.01)	0.15 (0.12 – 0.18)	0.08 (0.06 – 0.10)
Cerebellum (n = 12)	Cerebellar hemisphere (n = 8)	0.01 (0.00 – 0.01)	0.03 (0.02 – 0.04)	0.08 (0.02 – 0.13)
	Cerebellar vermis (n = 4)	0.02 (0.01 – 0.02)	0.12 (0.12 – 0.12)	N.A.
Brainstem (n = 22)	Midbrain (n = 6)	0.01 (0.00 – 0.01)	0.11 (0.04 – 0.26)	0.15 (0.13 – 0.20)
	Pons (n = 8)	<0.01 (0.00 – 0.01)	0.05 (0.04 – 0.06)	0.18 (0.12 – 0.21)
	Medulla (n = 8)	0.01 (0.01 – 0.03)	0.09 (0.06 – 0.16)	0.09 (0.06 – 0.11)
Other (n = 8)	Corpus callosum (n = 4)	0.01 (0.00 – 0.03)	0.23 (0.09 – 0.43)	N.A.
	Perforating floor of third ventricle (n = 4)	<0.01 (0.00 – 0.01)	N.A.	N.A.

N.A. = Not applicable.

Table sourced from Marcus et al.

The authors then focused specifically on the Circle of Willis, and attempted to characterize dissection forces that did or did not result in injury to the surrounding tissue. Results found that the force exerted during sharp and blunt dissection were significantly different (0.03N compared to 0.22N). It also found that the difference in force between sharp dissection maneuvers that did and did not result in injury were much smaller than the difference between blunt dissection maneuvers that did and did not result in injury. A box plot illustrating this data can be seen below.

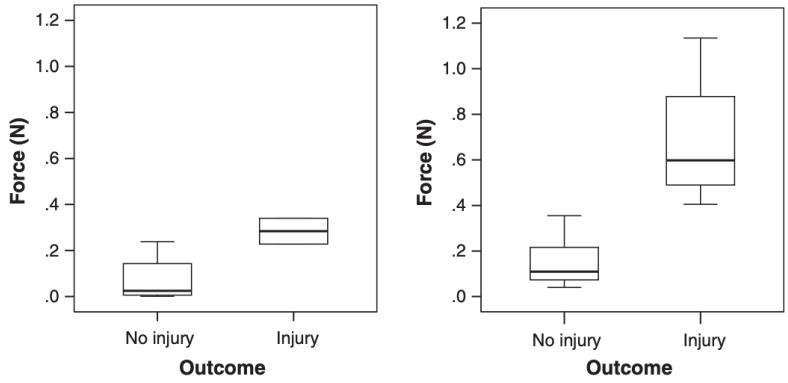

Figure 3. Box plot illustrating the median forces exerted (Newton) during (A) sharp and (B) blunt dissection around the Circle of Willis, stratified according to whether they did or didn't result in iatrogenic injury

Chart sourced from Marcus et al.

This data appears promising for our purposes of repositioning a retractor. Upon initial estimates, the adjustment in angle likely to occur using our device is unlikely to reach the threshold of injury of blunt dissection. With that said, this paper would have been more effective if it spent more time examining the force threshold of injury rather than just the average force in injury and noninjury events. Also this specific data comes from examination of forces on only the Circle of Willis, and could have been expanded to other parts of the brain.

Additionally, the authors note that other research indicates that the use of freshly acquired cadaver brains produces data likely generalizable enough to be valid in in vivo brains. However, the whole study takes place using only two specimens. It's difficult to believe that the brain model held the same integrity at the beginning of trials and after enduring 20 incisions in various areas.

Overall the study provides valuable numeric data to represent forces endured by the brain during microsurgery, and suggests that our design will fall under necessary force thresholds to cause trauma. However, more continuous data on trauma thresholds would have been more illuminating.

Improving the Precision and Speed of Euler Angles Computation

While small, inexpensive gyroscope and accelerometer chips have become somewhat ubiquitous in the past 10 years, they are not without their flaws. This paper seeks to quantify optimally efficient and accurate use of Micro-Electro-Mechanical systems by their representation of angles.

In order to locate the present orientation of our retractor and to input a new orientation via forcep angle mimicking control, we must make use of IMU sensors. Our size and budgetary requirements limit our accessibility to high-end gyroscope technology. However, according to Janota et al., the interpretation of the angular velocity readings can greatly affect the accuracy and speed of angle computation.

In order to determine accuracy and computational complexity of angular velocity interpretation, the authors generated sample gyroscope data for 120 seconds of simulated motion. They then interpreted gyroscope output into three different angle representations: rotation matrices, quaternions, and euler angles. Both rotation matrices and quaternions were calculated both using a precise and fast method, resulting in varying speed and accuracy assessments. Accuracy of each method is detailed in the figures below.

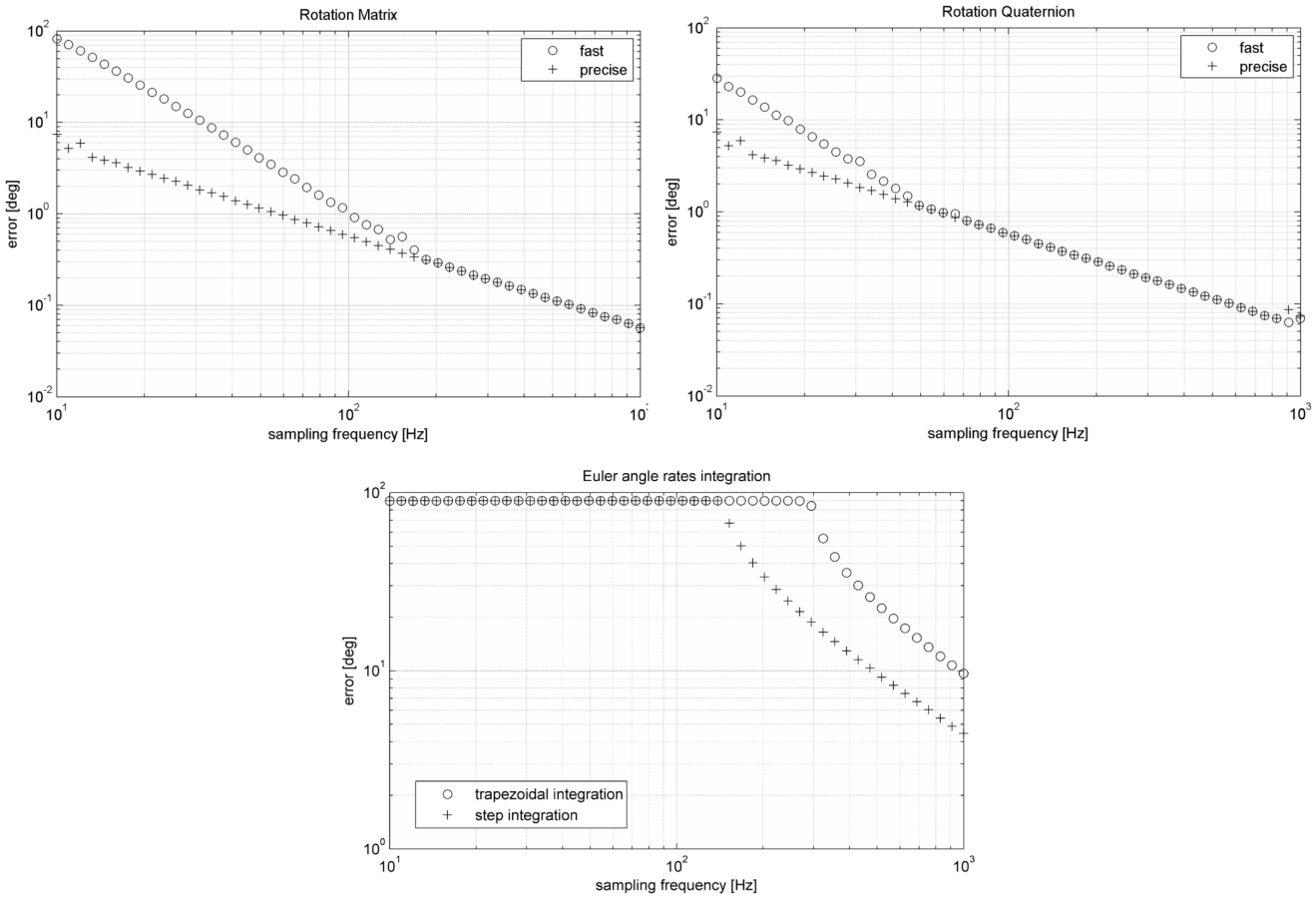

All graphs sourced from Janota et al.

The researchers also assessed gyroscope drift over time, and compared it to gyroscope data corrected by secondary sensor (accelerometer) readings. The data was combined using the following algorithm to determine the drift of the gyroscope as shown below. The figure demonstrates the necessity of secondary sensor data to correct gyroscope drift.

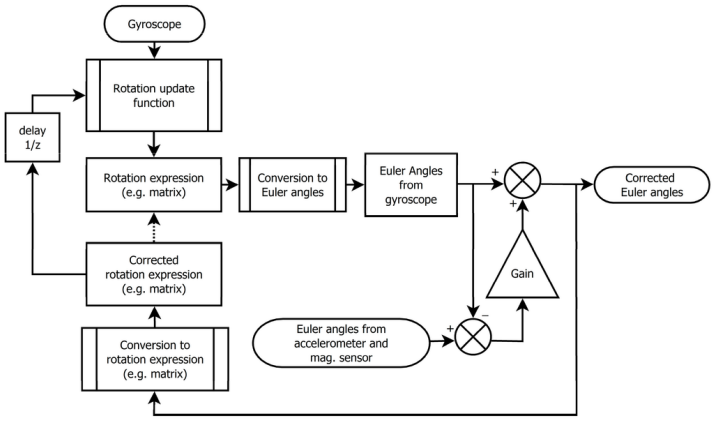

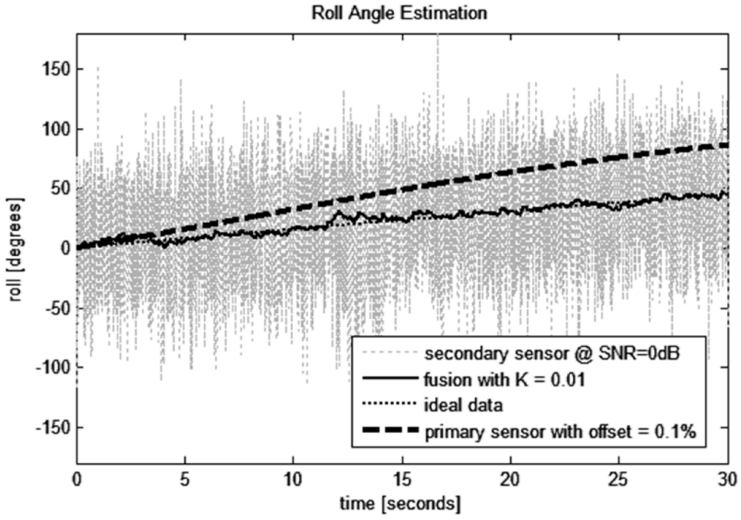

In the end, the paper concludes efficiency and accuracy data of angle representations as follows using an 8 bit microcontroller.

Table 1. Comparison of methods in terms of 8-bit AVR processor clock cycles.

Algorithm	Updating of the Rotational Matrix	Integration of the Euler Angle Rates	Updating of the Quaternion
Redundancy (count of variables)	**9	****3	***4
Gyroscope data processing (rotation update)	*** + 17,230 (6034 +)	***14,750	****11,462 (5120 +)
Normalization	**12,265	*****0	****1972
Vector transformation	****2301	*15,231 3)	***4321
Transformation to the rotational matrix	*****0	**12,930	****3536
Transformation to Euler angles	****7820	*****0	***10,673
Transformation to quaternion	***3370	**13,020	*****0
Clock cycles for the gyroscope-only system 1)	37,315 (26,119 +)	14,750	24,107 (17,765 +)
Clock cycles for the compensated system 2)	40,281 (29,085 +)	29,981 3)	39,476 (33,134 +)

Table 3. Accuracy of the algorithms.

Sampling Frequency	Maximal Error of the Algorithm during 120 s of Simulated Movement				
	Matrix-Based Algorithm		Integration of Euler Angle Rates	Quaternion-Based Algorithm	
	Fast	Precise	Step Integration	Fast	Precise
10 Hz	>180°	8°	>180°	30°	8°
50 Hz	4°	1°	>180°	1°	1°
100 Hz	1°	0.6°	>180°	0.6°	0.6°
500 Hz	0.1°	0.1°	8°	0.1°	0.1°
1000 Hz	0.06°	0.06°	4°	0.06°	0.06°

The conclusions of the study concisely show the accuracy and efficiency demands of each angle representation, and how they are dependent on sampling frequency of the gyroscope. This can easily be applied to our data collection, which requires high accuracy, but has generally little need for computational efficiency. Little can be improved in terms of the data acquisition or interpretation done in this paper. However, the author could have included more information on the specific model of gyroscope and accelerometer used.

Works Cited

White, Tim et al. “Frameless Stereotactic Insertion of Viewsite Brain Access System with Microscope-Mounted Tracking Device for Resection of Deep Brain Lesions: Technical Report.” *Cureus* vol. 9,2 e1012. 4 Feb. 2017, doi:10.7759/cureus.1012

Marcus HJ, Zareinia K, Gan LS, Yang FW, Lama S, Yang GZ, Sutherland GR. “Forces exerted during microneurosurgery: a cadaver study.” Int J Med Robot. 2014 Jun;10(2):251-6. doi: 10.1002/rcs.1568. Epub 2014 Jan 16. PMID: 24431265; PMCID: PMC4377085.

Janota A, Šimák V, Nemec D, Hrbček J. Improving the Precision and Speed of Euler Angles Computation from Low-Cost Rotation Sensor Data. *Sensors*. 2015; 15(3):7016-7039. https://doi.org/10.3390/s150307016